

1 **Multiple parallel expansions of bilaterian-like phototransduction gene families in the**
2 **eyeless Anthozoa**

3
4 Stacey Hansen¹, Meghan Payne¹, Kyle J McCulloch¹

5
6
7 1. Department of Ecology, Evolution and Behavior, University of Minnesota, St. Paul MN, 55108

8
9 Corresponding author: Kyle J McCulloch, mccu0232@umn.edu

10
11
12
13 **Abstract**

14 Opsin-mediated phototransduction cascades in photoreceptor cells are primarily responsible for
15 light-mediated behaviors in animals. Although some visual cascades are well-studied,
16 phototransduction mediated by non-visual opsins and in non-model animal lineages are poorly
17 characterized. In the Cnidaria (jellyfish, corals, sea anemones etc.), the sister group to Bilateria
18 (vertebrates, arthropods, mollusks etc.), limited evidence suggests some overlap with bilaterian
19 phototransduction. This raises the question of whether phototransduction pathways arose a
20 single time early in animal evolution or if light signaling cascades have evolved multiple times.
21 These evolutionary patterns remain obscured because almost nothing is known about
22 phototransduction in a major group within Cnidaria, the eyeless Anthozoa (corals, sea
23 anemones, sea pens etc.). To better understand whether bilaterian-like phototransduction could
24 be present in Anthozoa, we phylogenetically characterized 63 genes in 12 protein families
25 known to be crucial in two types of bilaterian phototransduction in the sea anemone
26 *Nematostella vectensis*. Using high quality genomic data from *N. vectensis*, we took a candidate
27 gene approach to find phototransduction genes and characterize their expression in
28 development and regeneration. We found that *N. vectensis* possesses the core suite of proteins
29 for both r-opsin and c-opsin mediated phototransduction. In addition, several new gene
30 subfamilies were identified, particularly in the G protein subunits and TRP channels, and many
31 were anthozoan-specific. We identified a novel G protein α subunit family, which we call GaVI,
32 and characterized its expression in *N. vectensis* with *in situ* hybridization. This expansion of
33 phototransduction genes correlates with a large anthozoan-specific radiation in opsin number,
34 suggesting possible coevolution of receptor and signaling diversity in Anthozoa. While further
35 functional experiments on these genes are needed, our findings are in line with the hypothesis
36 that the common ancestor of Eumetazoa had at least two related phototransduction cascades
37 which then further diversified in each animal lineage.

39 1. Introduction

40

41 Nearly all animals utilize opsin-based light-sensing in a wide variety of contexts for survival and
42 reproduction (Terakita, 2005). This type of light sensing is mediated at the cellular level by
43 specific G protein signaling cascades in photoreceptor cells, known as phototransduction
44 cascades (Shichida and Matsuyama, 2009; Yau and Hardie, 2009). Opsins are part of the G
45 protein-coupled receptor (GPCR) superfamily, and together with a vitamin A derived
46 chromophore are termed rhodopsins (Okada et al., 2004; Palczewski et al., 2000). Upon
47 absorbing a photon of light, the rhodopsin complex activates G protein signaling in the cell via
48 its specific binding to a particular $G\alpha$ subunit in the G protein complex (Simon et al., 1991; Yau
49 and Hardie, 2009). There are at least 4 known pathways that can be defined by the opsin and G
50 protein complex that initiate the cascade in a cell (Fain et al., 2010). The best studied cascades
51 are associated with the ciliary opsins (c-opsins) and rhabdomeric opsins (r-opsins). C-opsins
52 are best known in the context of vertebrate rods and cones, signaling through a specific G
53 protein complex termed transducin ($G\tau$), a phosphodiesterase (PDE), the second messenger
54 cGMP, and cyclic nucleotide gated (CNG) channels (Lamb, 2013; Yau, 1994). In contrast, r-
55 opsins are best known from microvillar regions of rhabdomeric photoreceptor cells in the
56 compound eyes of insects (Wang and Montell, 2007). The r-opsin phototransduction cascade
57 utilizes a $G\alpha_q$ class subunit, and signals through a phosphoinositide pathway involving
58 phospholipase C (PLC) and transient receptor potential (TRP) channels (Hardie and Raghu,
59 2001; Katz and Minke, 2009; Wang and Montell, 2007).

60

61 While these pathways are elucidated in a limited number of contexts, phototransduction by
62 canonical opsins in non-model organisms and by non-typical opsin groups is poorly understood
63 (Arendt et al., 2004; Gornik et al., 2021; Hattar et al., 2003; Kozmík et al., 2008; Liegertová et
64 al., 2015; Mason et al., 2012; Rawlinson et al., 2019; Velarde et al., 2005; Vöcking et al., 2022,
65 2017). This limits our understanding of the evolution of this pathway and visual systems more
66 broadly. Was a single phototransduction cascade assembled once and was modified throughout
67 animal evolution, or did multiple cascades *de novo* evolve independently to function in different
68 contexts? It is thought that opsins evolved early in animals and that multiple classes of opsins
69 were already present before the split of Bilateria and Cnidaria (Arendt et al., 2004; Ramirez et
70 al., 2016; Schnitzler et al., 2012). Opsin photoreceptive functions have been conserved across
71 animals, suggesting signaling cascades may also share an early animal origin. This is
72 supported by investigating the “non-visual” tetraopsins, xenopsins and cnidopsins, where the

73 limited data available suggest all or part of the cascade is similar to either r- or c-opsin cascades
74 (Döring et al., 2020; Kayal et al., 2018; Kojima et al., 1997; Koyanagi et al., 2008; Kozmik et al.,
75 2008; Liegertová et al., 2015; Plachetzki et al., 2012, 2010; Vöcking et al., 2017). To better
76 understand the evolution of phototransduction cascades, we need to understand more about the
77 pathways in animals outside of model bilaterians.

78

79 Cnidaria are sister to Bilateria and offer an important phylogenetic comparison to understand
80 the evolution of complexity in animals. The few comparative studies on phototransduction in
81 Cnidaria have almost exclusively focused on jellyfish and *Hydra* (Medusozoa) (Ekström et al.,
82 2008; Plachetzki et al., 2010; Vöcking et al., 2022) Evidence in box jellies suggests that a Gαs
83 subunit signals via the non-canonical AC enzyme, similar to bilaterian tetraopsin signaling
84 (Koyanagi et al., 2008). In addition, cnidarians with eyes share many of the same molecular
85 components as bilaterian eyes, such as developmental genes, phototransduction cascade
86 members, and opsins (Kozmik et al., 2008). These similarities suggest that the genetic
87 components could have assembled in a signaling pathway and associated with opsins before
88 the split of Bilateria and Cnidaria. Conversely the mechanisms of light sensing in the other major
89 cnidarian group, the eyeless Anthozoa, have received relatively little attention (Mason et al.,
90 2012). A more complete view of anthozoan phototransduction will provide important
91 comparative data with both Medusozoa and Bilateria, and could better elucidate how and when
92 different cascades arose.

93

94 The emerging model sea anemone *Nematostella vectensis* is an anthozoan cnidarian that lives
95 in shallow estuaries of brackish water and salt marshes (Layden et al., 2016). Development
96 proceeds from egg to free-swimming larval stage known as the planula by about 48 hours at
97 room temperature, then undergoes metamorphosis into a juvenile primary polyp with four
98 tentacles after roughly ten days (Layden et al., 2016). The primary polyp grows in a nutrient
99 dependent matter and is sexually mature by about 3 months. *N. vectensis* can also reproduce
100 asexually via transverse fission and has robust adult whole-body regeneration. Mature *N.*
101 *vectensis* adults have two germ layers and a mouth that is surrounded by up to sixteen
102 tentacles (Layden et al., 2016). Rather than specialized organs like an eye, specialized cell
103 types are dispersed throughout the animal, including opsin-expressing cells (Layden et al.,
104 2016; McCulloch et al., 2023).

105

106 Though *N. vectensis* is eyeless, larval dispersal, adult locomotor activity, and sexual
107 reproduction are all light-dependent (Layden et al., 2016; Tarrant et al., 2019). *N. vectensis* also
108 has among the highest number of opsins found in animals, at 29 (McCulloch et al., 2023).
109 Additionally, *N. vectensis* have opsins from three groups: cnidopsins, which are sister to
110 bilaterian xenopsins, the **Anthozoan Specific Opsins II** (ASO-II) which are sister to canonical
111 visual c-opsins, and the **Anthozoan Specific Opsins I** (ASO-I) which are sister to all other animal
112 opsins (Fig. 1B) (McCulloch et al., 2023). In contrast, medusozoans only have one opsin class,
113 the cnidopsins, which are not sister to c- or r-opsins, making it a challenge to compare these
114 pathways without direct orthology (Fig. 1B) (Macias-Munoz et al., 2019; Suga et al., 2008). The
115 anthozoan-specific opsin diversity could also be reflected in distinct signaling pathways present
116 in the variety of opsin-expressing cell types in *N. vectensis* (McCulloch et al., 2023).
117 Understanding the extent of conservation in phototransduction cascade proteins in *N. vectensis*
118 could help us trace the origins of the phototransduction cascade in animals.
119

120 Given that signals of at least partial conservation of phototransduction cascades are seen
121 across animals, we hypothesize *N. vectensis* would make use of these same conserved
122 pathways for phototransduction. The current study aims to identify the presence of orthologs of
123 known phototransduction cascade genes in *N. vectensis* as a first step in characterizing the
124 phototransduction cascade members in this understudied clade. We searched exhaustively for
125 the major components of known phototransduction cascades across major animal groups with
126 an emphasis on adding anthozoan representatives for each tree. We identify several lineage-
127 specific duplications among these highly conserved genes, many unique to Anthozoa. This is
128 the first attempt at characterizing phototransduction gene candidates in any anthozoan and an
129 important step toward functionally characterizing these genes in the future.
130

131 1. Material and Methods

133 2.1 Sequence Retrieval

134 Accession numbers for *Hydra vulgaris* candidate phototransduction genes were obtained from
135 Table 1 of (Macias-Munoz et al., 2019) and their coding sequences were retrieved from NCBI
136 GenBank. To find the *N. vectensis* candidate proteins, BLASTx searches were performed using
137 the *H. vulgaris* coding sequences as bait into the *N. vectensis* annotated proteins from the v2
138 genome in Geneious (Altschul et al., 1990; Zimmermann et al., 2020). Reciprocal BLAST
139 searches were performed for each top query hit into the *Hydra vulgaris* v2 mRNA gene model. If

140 the top query hit was not the same, reciprocal BLAST searches were repeated until the same
141 result was obtained, and all results were added. For each search, the top hits with significant
142 percent similarity (>60%) and query coverage (>50%) were saved.

143

144 Following initial identification of *N. vectensis* candidate proteins, BLASTp searches were
145 performed on NCBI using the *N. vectensis* sequences as bait. The sequences were first
146 searched on the UniProtKB/Swiss-Prot (swissprot) data, followed by the Reference proteins
147 (refseq_protein) and non-redundant protein sequences (nr) if insufficient query hits were shown.
148 The *Nematostella vectensis* sequences were searched in the following taxa: *Mus musculus*
149 (taxid:10088), *Danio rerio* (taxid:7955), *Drosophila melanogaster* (taxid:7227), *Xenopus*
150 *tropicalis* (taxid:8364), *Mnemiopsis leidyi* (taxid:27923), *Trichoplax adherens* (taxid:10227),
151 *Crassostrea virginica* (taxid:6565), *Limulus polyphemus* (taxid:6850), *Octopus bimaculoides*
152 (taxid:37653), *Acropora millepora* (taxid:45264), *Exaiptasia pallida* (taxid:2652724), Cubozoa
153 (taxid:6137), Scyphozoa (taxid:6142), Hydrozoa (taxid:6074), Zoantharia (taxid:6102), and
154 Octocorallia (taxid:6132). The top 1-6 query hits for each taxon were manually selected for each
155 species from each *N. vectensis* candidate gene BLAST result. Redundant sequences with the
156 same accession numbers, identical protein sequences, and similar isoforms were removed.
157 When the *N. vectensis* sequences did not yield sufficient BLAST results for a species,
158 sequences found in other similar species were used as the bait. The *N. vectensis* candidate
159 protein sequences were also searched in the genome assemblies of *Alatina alata* (Ohdera et
160 al., 2019) and *Aurelia aurita* (Gold et al., 2019), and the top query hits were saved. Additional
161 sequences were obtained from alignments from (Krishnan et al., 2015; Lagman et al., 2022;
162 Moroz et al., 2023; Peng et al., 2015; Vöcking et al., 2022) and redundant sequences were not
163 included.

164

165 For the G protein \square genes, *N. vectensis* sequences were retrieved from Interpro (Paysan-
166 Lafosse et al., 2023) using the domain accession numbers PS50058 and PF00631. Adenylyl
167 cyclase sequences were retrieved from (Vöcking et al., 2022) and used as bait to search on
168 NCBI BLAST in the species listed previously.

169

170 **2.2 Alignments and Phylogenetic Tree Construction**

171 Amino acid sequences from the resulting hits were aligned with the *N. vectensis* candidate gene
172 sequences on Geneious Prime with the MAFFT Alignment v7.450 using default parameters
173 (Katoh and Standley, 2013).

174

175 Pseudo-maximum likelihood trees were generated from the MAFFT alignments using FastTree
176 v2.1.11 (Price et al., 2010) with default settings. These trees were reviewed to identify the
177 closest outgroups and to check that representative species were present in each clade within
178 each tree. Sequences falling outside of outgroups, orphans, and highly divergent sequences
179 were removed. When previously uncharacterized subclades within each gene tree were
180 identified in other animals but not *N. vectensis*, additional BLAST searches were performed and
181 added to the alignment. If newly added *N. vectensis* sequences were identified in the gene tree
182 but not in any known subclades, additional BLAST searches in the above species were
183 performed to confirm the presence or absence of orthologs in each animal lineage. Alignments
184 and FastTrees were made iteratively as sequences were added and removed to finalize the
185 trees.

186

187 Finalized alignments were realigned with MAFFT using the same settings as previously. For
188 each gene family, a maximum likelihood tree was constructed using IQtree2 (Minh et al., 2020)
189 on the Minnesota Supercomputing Institute's Agate cluster using the following command: iqtree
190 -s <ALIGNMENTNAME.phy> -st AA -nt AUTO -v -m TEST -bb 1000 -alrt 1000. This allowed for
191 auto-choosing the best model of protein evolution for each tree, based on the lowest likelihood
192 score from the Bayesian Information Criterion test. IQtree results yield both UltraFast bootstrap
193 (UFbs) and aSH-LRT support values. Branches are considered highly supported with 80% aSH-
194 LRT /95% UFbs support and were represented with a red circle on the Figures. Tree Figures
195 were created using iTOL and inkscape (Letunic and Bork, 2021). Species icons for Placozoa
196 and Porifera were obtained from phylopic.

197

198 **2.3 *In situ* Hybridization**

199 The G protein α subunit VI probe was generated from a PCR product on *N. vectensis* cDNA,
200 using the primer pair: Fwd:ATTCAGGCAAAAGCACGTTT Rev:GGGATGCGAAAAATACCACC.
201 The PCR product was ligated to pGEM-T Easy vector backbone (Promega) and DIG-labeled
202 RNA probes were synthesized using T7 megascript kit (Ambion) and cleaned up using a Zymo
203 RNA cleanup kit, according to previously published methods (McCulloch et al., 2023). *In situ*
204 hybridization was performed using a standard *N. vectensis* protocol as previously published
205 (McCulloch 2023). Animals were mounted on a microscope slide and chromogenic staining was
206 visualized with a Nikon90i using DIC optics.

207

208 **2.4 mRNA Expression Patterns**

209 *N. vectensis* phototransduction candidate proteins that were confirmed phylogenetically were
210 then identified on the *N. vectensis* embryonic and regeneration transcriptome database,
211 NvERTx.4 (Warner et al., 2018) using tBLASTn default parameters. The result with 100% match
212 was selected and the regeneration expression data was retrieved. Developmental expression
213 data was retrieved from previously published transcriptomic data (McCulloch et al., 2023). For
214 details on the assembly and mapping methods please refer to the original references
215 ((McCulloch et al., 2023; Warner et al., 2018) The regeneration data is in normalized “counts,”
216 available on NvERTx, while the developmental time series is shown in normalized TPM.

217

218 **2. Results and Discussion**

219 Opsins evolved early in animals and are present in nearly all major groups (Fig. 1A,B).
220 Canonical ciliary and rhabdomeric phototransduction cascades make use of distinct opsins and
221 other proteins in the pathway (Fig. 1C,D). Although c- and r- pathways are best known in
222 vertebrates and insects respectively, both animal lineages have components of both pathways
223 (Table 1). A summary of *N. vectensis* and *H. vulgaris* c- and r- pathway members show both
224 cnidarian species also have the core components of these pathways (Table 1). Expression
225 levels of all the transcripts identified in this study during regeneration and embryonic
226 development are summarized in heatmaps (Fig. 2).

227

228 **3.1 Initiation of the phototransduction cascade**

229 All phototransduction cascades across animals are initiated by a rhodopsin absorbing light and
230 activating the associated heterotrimeric G protein, constituted of an α , β , and γ subunit. Upon
231 photon absorbance, the α separates from the β and γ subunits, and functions as a GTPase to
232 activate an effector enzyme, which can differ depending on the type of phototransduction
233 cascade (Shichida and Matsuyama, 2009).

234

235 **3.1.1 Heterotrimeric G protein**

236 The α subunit is the most studied of the G protein complex. Best known for activating cGMP
237 phosphodiesterase (PDE) in ciliary opsin cells and for activating phospholipase C (PLC) in
238 rhabdomeric opsin cells. While the β and γ subunits participate in regulation of the cascade,
239 much less is known about their function in any phototransduction cascade outside of
240 vertebrates.

241

242 G α subunit

243 There are five known major groups of G α subunits in animals, of which three are known to be
244 involved in phototransduction (Lokits et al., 2018). Within these major groups, duplications and
245 subsequent lineage-specific G α subunits have evolved, such as the vertebrate G α t, which is a
246 duplicate of the ancestral G α i group (Lagman et al., 2012). Well-studied pathways involve the
247 G α q protein which activates the r-opsin signaling cascade, and the G α i/G α t family found in
248 retinal rods and cones (Shichida and Matsuyama, 2009).

249

250 We surprisingly found that *N. vectensis* has 6 G α orthologs, five in the families G α s, G α o, G α q,
251 G α i, G α 12, and one in a highly supported novel clade within the G α tree (Fig. 3A, Fig. S1). Our
252 tree places this group sister to the G α q and G α 12 clade, although this relationship has low
253 support. Domain analysis reveals that this unspecified *N. vectensis* gene retains the
254 diphosphate binding (P-) loop (GXGESGKS), Mg²⁺ binding domain (RXXTXGI and DXXG), and
255 guanine ring-binding motifs (NKXD and TCAT) within the GTPase domain characteristic of G α
256 protein structure (Oldham and Hamm, 2006). An ortholog of this gene was previously identified
257 in the coral *Acropora palmata*, though no phylogenetic classification was attempted (Mason et
258 al., 2012). Our novel gene is highly conserved with this coral G α . We identify additional
259 anthozoan representatives in this new clade, but unexpectedly we also found multiple spiralian
260 sequences and a single ortholog in *Branchiostoma belcheri* (Fig. 3A, Fig. S1). However no
261 results were found for any ecdysozoan, any other deuterostome, or any medusozoan. Because
262 the gene is present in both Cnidaria and Bilateria, this novel clade was likely present in their
263 common ancestor and subsequently lost in other animal lineages. We propose to refer to this
264 sixth group as G α VI.

265

266 To identify expression patterns of this novel gene in *N. vectensis* development, *in situ*
267 hybridizations were performed (Fig. 3B-F). We find that early in gastrulation, NvG α VI expression
268 is concentrated in the pre-endodermal plate, and continues throughout gastrulation as this
269 invaginates and the endoderm is formed (Fig. 3C-D). Later, in the larval planula stages, NvG α VI
270 is expressed broadly in the endoderm and specifically in the ectodermal lip where the cells
271 begin to internalize and form the pharynx (Fig. 3E-F). Expression is also seen in later planula
272 stages in the sensory apical organ (arrowheads, Fig. 3F). No expression could be seen in later
273 stages although RNA-seq data suggest some expression in developing and regenerating polyps
274 (Fig. 2). Some opsins are known to be expressed near the mouth and in the apical organ at

275 these stages, including *NvASOII-8b* and *NvASOI-2* (McCulloch 2023), however it is still
276 unknown whether there is a functional link between this novel GαVI subunit and opsins.

277

278 G proteins are involved in many types of cellular signaling so we cannot rule out that these
279 orthologs may be used for functions other than photoreception. However evidence of multiple
280 Gα family members in cnidarian phototransduction suggests these might function in *N.*
281 *vectensis* phototransduction as well. The Gas protein of the box jelly *Tripedalia cystophora* may
282 regulate cAMP concentrations in response to light (Koyanagi et al., 2008). In the coral *A.*
283 *palmata*, two ASO-II opsins were capable of activating the *A. palmata* Gαq ortholog, while one
284 of these could activate the unspecified Gα protein that we now classify as the novel GαVI
285 (Mason et al., 2012). *N. vectensis* has 15 ASO-II paralogs and 12 cnidopsin paralogs, so it is
286 possible some of these could use Gas, Gαq, or GαVI for phototransduction.

287

288 Gβ subunit

289 Five major Gβ subunits are known in animals, including Gβ1 expressed in rod photoreceptors,
290 Gβ3 (β-transducin) expressed in cone photoreceptors (Dexter et al., 2018; Peng et al., 1992).
291 Our tree aligns with previous research showing that Gβ homologs are split into two major clades
292 in animals: Gβ5, and Gβ1 which has been duplicated multiple times in vertebrates (Gβ1-4) (Fig.
293 S2). Similar to protostomes, we found that *N. vectensis* has one homolog in each of these major
294 clades (Fig. S2). In contrast to *N. vectensis*, *H. vulgaris* has three closely related copies of the
295 gene within the Gβ1-4 group which likely arose from species-specific duplications of the *H.*
296 *vulgaris* Gβ1 gene.

297

298 G□ subunit

299 At least 12 G□ subunit genes have been identified in vertebrates. The GNG cluster contains 2
300 deuterostome-specific subgroups with 8 paralogs among vertebrates, and a single ortholog in
301 protostomes (Krishnan et al., 2015). One GNG13 ortholog is typically present in all animals
302 except sponges and ctenophores, while the G□ transducin (GNGT) family is vertebrate specific.
303 Previous work identified 2 *N. vectensis* genes in the GNG cluster and 1 GNG13 homolog
304 (Krishnan et al., 2015).

305

306 Using domain searches in Pfam rather than BLAST, we confirmed that *N. vectensis* has the 3
307 G□ genes previously identified and identified 2 additional G□ sequences (Fig. 4, Fig. S3).
308 These fall into two subgroups outside of the previously identified G□ subclades. One sequence

309 is in a cnidarian-specific group where the three *Hydra* duplicates are found, and another is
310 found in an anthozoan-specific group. Whether the novel G \square subgroups are sister to the
311 established groups is not highly supported, however the topology placing all of these in a single
312 clade is highly supported (Fig. 4).

313

314 One of the reasons for this uncertainty is the short sequence length of the G \square gene (49-75
315 amino acids long for the *N. vectensis* genes), which makes phylogenetic inference a challenge.
316 To confirm that the unspecified *N. vectensis* G \square genes might still have G protein function, we
317 analyzed the *N. vectensis* sequences using InterPro database functional domain scans in
318 Geneious. This analysis predicted intact G \square functional domains, confirming these could likely
319 function in the heterotrimeric complex with other G protein α and β subunits. While the
320 relationships between these different G \square genes is not certain, we show that *N. vectensis* has
321 more G \square subunits than previously identified.

322

323 Previous research has shown both interchangeability and specificity in \square subunits with evidence
324 that G \square subunit identity is not important in some signaling contexts *in vivo*, while in other cases
325 a particular G \square subunit is required for a specific function (Dexter et al. 2018). It is thus possible
326 the multiple *N. vectensis* G \square genes may be similar, both functioning in specific G $\beta\gamma$ complexes
327 for particular phototransduction cascades and also others that are interchangeable in other G
328 protein signaling contexts.

329

330 **3.1.2 Effector enzymes**

331 After activation by the G α subunit, effector enzymes such as cGMP-PDE and PLC affect the
332 concentrations of second messengers. Other effector enzymes include guanylyl cyclase (GC) in
333 Gao-opsin signaling in the ciliary photoreceptors of scallops (Del Pilar Gomez and Nasi, 2000)
334 and adenylyl cyclase (AC) in chicken Gai signaling via neuropsins (tetraopsins) in non-typical
335 photoreceptor cells of the retina and brain (Yamashita et al., 2010). AC has also been
336 implicated in Gas signaling in box jelly phototransduction (Koyanagi et al., 2008).

337

338 Phospholipase C

339 In *Drosophila*, PLC β 4 hydrolyzes phospholipid phosphatidylinositol 4,5-bisphosphate (PIP2) to
340 inositol 1,4,5-triphosphate (InsP3) and diacylglycerol (DAG) upon activation by G α q (Hardie and
341 Raghu, 2001). These molecules both act as second messengers to change the concentrations
342 of calcium and other metabolites within the cell, leading to the opening of transient receptor

343 potential channels (TRPs). We show that *N. vectensis* has the same two orthologs as the
344 *Drosophila* PLC β genes (Fig. S4). The presence of both a Gaq gene and PLC β 4 homolog
345 shows that *N. vectensis* have the necessary components to utilize a signaling pathway similar to
346 that of the rhabdomeric pathway.

347

348 Cyclic GMP-Phosphodiesterase (cGMP-PDE)

349 In vertebrate retinal ciliary photoreceptors, the active cGMP-PDE6 complex increases levels of
350 the second messenger cGMP, which then closes cyclic nucleotide gated (CNG) channels in the
351 plasma membrane. The vertebrate PDE6 is made up of one α subunit, one catalytic β subunit,
352 and two inhibitory γ subunits. The group sister to the vertebrate PDE6 subunits contains the
353 single *Drosophila* cGMP-specific PDE6 ortholog. Cnidarians appear to also have an ortholog to
354 PDE6, but this is unclear due to low support (Fig. S5). If PDE6 signaling is a vertebrate-specific
355 innovation, *N. vectensis* could be more similar to invertebrate c-opsin signaling, with ASO-II
356 opsins signaling through GC rather than PDE6.

357

358 Guanylyl Cyclase

359 The guanylyl cyclase (GC) enzyme family is split into transmembrane and soluble subfamilies.
360 The transmembrane GCs, also called atrial natriuretic peptide receptors (ANPR), can activate or
361 inhibit phototransduction via calcium- and cGMP-dependent feedback loops (Dizhoor et al.,
362 1994; Koch and Stryer, 1988). The transmembrane GCs in vertebrate phototransduction are
363 part of a vertebrate-specific subfamily called retinal GCs while evidence from scallop suggests
364 an ANPR subfamily member is involved in phototransduction (Del Pilar Gomez and Nasi, 2000;
365 Potter, 2011). We found that *N. vectensis* has 3 transmembrane GC genes and 6 soluble GC
366 genes (Fig. 5A, Fig. S6). One of these NvGC paralogs is in a cnidarian-specific group sister to
367 the bilaterian ANPR family, while the other two are found in two additional cnidarian- and
368 anthozoan-specific groups within the transmembrane GCs (Fig. 5B). We hypothesize that the
369 NvANPR could function in a conserved role in phototransduction like the scallop ANPR,
370 potentially in NvASO-II (c-opsin-related) expressing cells. The functions of the cnidarian
371 transmembrane GCs are unknown. However gene expansions in the GC and other
372 phototransduction-related gene families could correlate with the expanded set of *N. vectensis*
373 opsins and be used for different phototransduction contexts.

374

375 Adenylyl cyclase

376 While cGMP is the most studied secondary messenger in vertebrate c-opsin signaling, cAMP
377 signaling via AC5/6 has been suggested as having a major role in the ancestral chordate
378 phototransduction cascade (Lamb and Hunt, 2017). Recent evidence points to this with a role of
379 cAMP in vertebrate r-opsin signaling. In mice, AC2 is activated by Gaq in the melanopsin
380 pathway (Chen et al., 2023). In the box jelly *T. cystophora*, a cnidopsin-Gαs pathway activates
381 an AC enzyme that affects cAMP concentrations (Koyanagi et al., 2008). It is currently unknown
382 which specific AC type is involved, however AC3 has been suggested due to the similarities
383 between the jellyfish phototransduction cascade and the vertebrate olfactory signaling cascade
384 (Firestein, 2001).

385

386 We found that *N. vectensis* has homologs of AC types 5/6, 3, and 9 (Fig. 5A). This confirms
387 previous research indicating cnidarians only have these three AC types (Vöcking et al. 2022).
388 AC3 and AC5/6 are likely candidates in the phototransduction cascade in *N. vectensis*, possibly
389 through cnidopsin signaling. Overall, patterns of GC and AC participation in various
390 phototransduction cascades suggest that these enzymes can be repeatedly recruited and
391 swapped for one another over the course of animal evolution. Their prevalence across several
392 types of phototransduction cascade suggests they were recruited early while the vertebrate c-
393 opsins cascade relying on PDE6 may be a later innovation.

394

395 **3.1.3 Ion Channels**

396 When effector enzymes alter the concentrations of second messengers, ion channels open or
397 close in response, leading to voltage changes and propagation of the light signal. In c-opsin
398 expressing ciliary photoreceptors, these are CNG channels while r-opsin expressing
399 rhabdomeric photoreceptors utilize TRP channels.

400

401 Cyclic nucleotide gated (CNG) channels

402 CNG channels are thought to be the ancestral ion channel used in phototransduction before the
403 radiation of metazoans (Lagman et al., 2022). Dependent on the type of signaling, CNG
404 channels are either opened or closed in response to cascade activation (Fain et al., 2010).
405 Generally, three α subunits and one β subunit are used to assemble the channel, and these can
406 be mixed and matched (Lagman et al., 2022). There are six subunits of CNG channels in
407 animals, and anthozoans have the most of any animal group with five (Lagman et al. 2022). We
408 confirm that one subunit, CNGE, is anthozoan-specific (Fig. 6, Fig. S7). CNG channels are likely

409 involved in *N. vectensis* phototransduction, as *Hydra magnipapillata* CNG channels are
410 implicated in the contractile photo-response (Plachetzki et al., 2010).

411
412 Given these subunits form heterotetrameric channels in other animals, the large number of
413 subunits found in Anthozoa could allow for high combinatorial diversity of CNG channels and
414 their functional contexts. Our bulk RNA-seq data shows that CNG subunits are among the lower
415 expressing transcripts in both development and regeneration (Fig. 2). However *N. vectensis*
416 single cell transcriptomic data shows multiple subunits were co-expressed in the same cell
417 types in nearly all tissue types, including neural and glandular cell types (Lagman et al., 2022;
418 Seb  -Pedr  s et al., 2018). Together this suggests CNG subunits are not highly expressed in
419 bulk RNA-seq data because they are expressed in relatively fewer specialized cell types, and
420 distinct combinations could be specifically expressed in sensory and photoreceptor cell types.

421
422 Transient receptor potential channels
423 TRPC channels are the main type of TRP channel in *D. melanogaster* r-opsin
424 phototransduction, which open in response to cascade activation (Montell, 2005). TRP channels
425 are known to be involved in a variety of sensory contexts in animals and may have been co-
426 opted specifically into the r-opsin/Gq phototransduction cascade more recently in protostomes
427 (Plachetzki et al., 2010), although without more functional studies in Cnidaria, especially
428 Anthozoa, we cannot rule out a loss of Gq/TRP signaling in vertebrates.

429
430 We focused on TRPC channels which are the only TRPs known to be involved in
431 phototransduction. Our phylogenetic analysis revealed a large anthozoan-specific expansion in
432 TRPC channel homologs. *N. vectensis* has a total of 8 TRPC genes, while *H. vulgaris* has one
433 TRPC gene (Fig. 7A, Fig. S8) (Peng et al., 2015; V  cking et al., 2022). We find that previously
434 identified cnidarian TRPCs are split into two groups, one of which is pan-cnidarian, while the
435 other is anthozoan-specific (Fig. 7B, green and orange). The three *N. vectensis* TRPC genes
436 previously found and one additional novel paralog are all sister to bilaterian TRPC. We also
437 identified another anthozoan-specific TRPC group that falls sister to the previously defined
438 groups and has four additional *N. vectensis* sequences (Fig. 7B, blue). We show that *N.*
439 *vectensis* has multiple TRPC orthologs as part of either an anthozoan-specific expansion and
440 divergence or retention of ancient paralogs of this ion channel subfamily. *N. vectensis* could use
441 their many CNG and TRP channels in distinct signaling mechanisms, including potentially a
442 variety of distinct phototransduction contexts.

443

444 **3.2 Regulation of the phototransduction cascade**

445

446 G protein-coupled receptor kinases

447 The superfamily of G protein-coupled receptor kinases (GRKs) phosphorylate a variety of
448 GPCRs and includes the visual GRKs rhodopsin kinase (GRK1) and GRK7. GRK1 is
449 vertebrate-specific and has a role in recovery of the vertebrate ciliary phototransduction
450 cascade by phosphorylating rhodopsin and allowing the inhibitory arrestin protein to bind
451 (Lyubarsky et al., 2000). GPRK1 in *Drosophila* has a function analogous to vertebrate rhodopsin
452 kinase (Lee et al., 2004). However DmGPRK1 is phylogenetically placed with the β -adrenergic
453 receptor kinase group GRK2/3.

454 Another GRK, bovine GRK5 is expressed in the retina and can phosphorylate rhodopsin in a
455 light-dependent manner when expressed in insect cells (Premont et al., 1994). We found that *N.*
456 *vectensis* has homologs for both GRK5 and DmGPRK1, either of which could be involved in
457 regulating G protein-coupled receptor activity during the phototransduction cascade. We confirm
458 that GRK1 is vertebrate specific and that DmGPRK1 is included with the β adrenergic receptor
459 kinases GRK2/3 clade (Fig. S9).

460

461 Arrestin

462 Visual arrestin is an essential protein in the termination of visual signaling that inactivates
463 GPCRs and halts rhodopsin activity across Metazoa. Vertebrates have four arrestin proteins,
464 two of which function in phototransduction termination in rods and cones (Lamb et al., 2018;
465 Wilden et al., 1986). Protostomes have two arrestins with no 1:1 orthology with vertebrate
466 arrestins, one of which is involved in phototransduction (Gurevich and Gurevich, 2006;
467 Swardfager and Mitchell, 2007). In contrast, we identified only one arrestin gene in *N. vectensis*
468 and other cnidarians (Fig. S10). This cnidarian arrestin has been shown to function similarly to
469 bilaterian arrestins and plays a role in terminating G protein signaling in phototransduction
470 (Plachetzki et al., 2012). The presence of an arrestin protein with similar function in both
471 Bilateria and Cnidaria suggests that it has a highly conserved role in the termination of
472 phototransduction in animals, including *N. vectensis*.

473

474 Calcium binding proteins

475 Calcium ions have a variety of roles in G protein signaling, including in multiple
476 phototransduction cascades (Fain et al., 2010). Calcium-binding proteins regulate calcium ion

477 concentration and distribution, playing important roles in the regulation of phototransduction
478 (Ikura, 1996; Tanaka et al., 1995). The neuronal calcium sensor proteins are phylogenetically
479 and functionally related (Burgoyne and Weiss, 2001). Calmodulin is a calcium binding protein
480 that interacts with both CNG and TRP channels mediating positive and negative feedback
481 mechanisms (Babu et al., 1988; Bej and Ames, 2022; Sun et al., 2018; Trudeau and Zagotta,
482 2004). In vertebrates neurocalcin regulates the GC enzyme (Dizhoor et al., 1994) and
483 neurocalcin may also inhibits rhodopsin in fly eyes in a manner similar to recoverin in
484 vertebrates (Faurobert et al., 1996). We found that *N. vectensis* has orthologs for calmodulin
485 and neurocalcin, and two additional unspecified orthologs in the calcium binding family (Fig.
486 S11). Calmodulin is also the highest expressing transcript in both regeneration and
487 development (Fig. 2). It is possible that calmodulin and neurocalcin act in broad contexts for
488 calcium signaling in *N. vectensis*, including in phototransduction.

489

490 **Regulator of G protein signaling 9**

491 Regulator of G protein signaling (RGS) members of the R7 family (RGS6, RGS7, RGS9,
492 RGS11) form complexes with other proteins and act to regulate the phototransduction response
493 (Makino et al., 1999; Squires et al., 2018). We show that *N. vectensis* has RGS7 and RGS12
494 orthologs (Fig. S12). Pfam analysis reveals that the *N. vectensis* RGS7 maintains the functional
495 domains characteristic of the R7 family, which could allow it to regulate *N. vectensis*
496 phototransduction in a similar manner (Levay et al., 1999; Squires et al., 2018).

497

498 ***3.3 Expression of phototransduction genes in *N. vectensis****

499

500 Once we identified the phototransduction gene candidates in *N. vectensis*, we wanted to know
501 how they were expressed over both developmental and regeneration time (McCulloch et al.,
502 2023; Warner et al., 2018). Throughout development, calmodulin and the G protein α and β
503 subunits were among the highest expressing genes, including the novel GaVI (Fig. 7A). Many
504 TRP channels were also highly expressed, particularly the TRPV, TRPVL, and some TRPC
505 genes, qualitatively much more so than the CNG channels. This could indicate that TRP
506 channels have a broader role in multiple signaling contexts in the animal while CNG channels
507 might be more specifically expressed in fewer cell types. The cGMP-PDE δ subunit was also
508 very highly expressed, particularly during the planula stage of development potentially
509 correlated with sensory signaling specific to this swimming life stage, as some opsins are. Many

510 genes were also expressed during regeneration but none in obvious regeneration-specific
511 patterns (Fig. 7B).

512

513 **3.4 Discussion of *N. vectensis* phototransduction and evolutionary implications**

514

515 Our results reveal that similar components required for phototransduction in the major c-opsin
516 and r-opsin phototransduction cascades are present in the eyeless Anthozoa. We summarize
517 our results in Table 2 by showing the number of paralogs for each gene family in select species.
518 This aligns with the limited evidence from other cnidarians suggesting conserved
519 phototransduction components (Koyanagi et al., 2008; Kozmik et al., 2008; Vöcking et al.,
520 2022). Of note, *N. vectensis* consistently has more paralogs for most gene families relative to
521 *Hydra*, and this correlates with *N. vectensis* having more opsin receptor classes (3) than *Hydra*
522 (1). It is expected that vertebrates have more paralogs due to whole-genome duplications,
523 however *N. vectensis* has more than even vertebrates for some gene families (TRPC, GC) and
524 more than *D. melanogaster* for several gene families (TRPC, GC, ANPR, CNG, PDE, G \square). This
525 suggests that patterns of gene duplication leading to sub- and neofunctionalization are not
526 exclusive to Bilateria and occurred in parallel in Cnidaria. Further investigation in overlooked
527 lineages such as Anthozoa will continue to reveal previously unappreciated evolutionary history
528 and the origins of complexity among animals.

529

530 A novel G α subunit, G α VI, was also identified in Anthozoa and Spiralia (and *Branchiostoma*)
531 and is absent in the major vertebrate and ecdysozoan animal models. This suggests that losses
532 have occurred in these animal lineages, and a lack of attention in cnidarian and spiralian groups
533 left this subfamily previously unidentified. G proteins and their associated α subunits are
534 involved with a diverse range of signaling mechanisms, so this novel G α VI may have important
535 roles in these species including in phototransduction.

536

537 In Anthozoa, Medusozoa, and Bilateria, we see many of the same core phototransduction
538 pathway components (opsins, G α , effector enzymes, and channels). Some specific pathways,
539 such as vertebrate c-opsin/Gat signaling, have specialized by swapping paralogs or even
540 adding novel enzymes to the cascade. When compared alone, it is impossible to say whether
541 the highly specialized G α q/r-opsin pathway and the Gat/c-opsin pathway in insect and
542 vertebrate eyes are *de novo* evolved or share ancestry. Our findings along with evidence that
543 opsins diverged before the split of Bilateria and Cnidaria suggest that the phototransduction

544 cascades across Metazoa could have arisen in their earliest common ancestor. This is further
545 supported by similarities between medusozoan phototransduction and the vertebrate olfactory
546 transduction cascade (Firestein, 2001; Koyanagi et al., 2008; Ramirez et al., 2016). Our data
547 are in line with the hypothesis that the last common ancestor of animals had a general GPCR
548 signaling pathway before opsins and olfactory receptors split, which then diversified as new
549 sensory modalities evolved. With more sampling in new lineages and contexts, and with further
550 functional data in the future, we are closer to understanding the origin and continued evolution
551 of phototransduction in animals.

552

553 **4. Conclusions: Implications for the phototransduction cascade in *N. vectensis***

554 Current evidence suggests both opsins and their respective phototransduction cascades
555 evolved before the split of Bilateria and Cnidaria. By identifying well-known phototransduction
556 cascade members in *N. vectensis*, we show the first evidence that Anthozoa possess the
557 capacity to signal through similar cascades as Bilateria. Furthermore, by investigating a
558 relatively understudied lineage, we have identified novel subgroups in otherwise well-studied
559 gene families, such as GaVI and multiple novel G \square subunits, GC genes, and TRP channels in
560 *N. vectensis* and Anthozoa. More functional work must be done to confirm these genes work
561 together in a cascade. Even so, our findings highlight that broader taxonomic sampling in
562 otherwise well-known gene families can uncover previously unknown evolutionary history of
563 well-known proteins and pathways and potential novel functional diversity in animals.

564

565 **Acknowledgements**

566 We thank members of the Snell-Rood Lab for critical feedback on this manuscript. We also
567 thank the UMN University Imaging Centers for providing the training and equipment to obtain in
568 situ images.

569

570 **References**

571 Altschul, S.F., Gish, W., Miller, W., Myers, E.W., Lipman, D.J., 1990. Basic local alignment
572 search tool. *J. Mol. Biol.* 215, 403–410. [https://doi.org/10.1016/S0022-2836\(05\)80360-2](https://doi.org/10.1016/S0022-2836(05)80360-2)

573 Arendt, D., Tessmar-Raible, K., Snyman, H., Dorresteijn, A.W., Wittbrodt, J., 2004. Ciliary
574 photoreceptors with a vertebrate-type opsin in an invertebrate brain. *Science* (80-.). 306,
575 869–871. <https://doi.org/10.1126/science.1099955>

576 Babu, Y.S., Bugg, C.E., Cook, W.J., 1988. Structure of calmodulin refined at 2.2 Å resolution. *J.*
577 *Mol. Biol.* 204, 191–204. [https://doi.org/10.1016/0022-2836\(88\)90608-0](https://doi.org/10.1016/0022-2836(88)90608-0)

578 Bej, A., Ames, J.B., 2022. Retinal Cyclic Nucleotide-Gated Channel Regulation by Calmodulin.
579 *Int. J. Mol. Sci.* 23. <https://doi.org/10.3390/ijms232214143>

580 Burgoyne, R.D., Weiss, J.L., 2001. The neuronal calcium sensor family of Ca²⁺-binding
581 proteins. *Biochem. J.* 353, 1–12. <https://doi.org/10.1042/bj3530001>

582 Chen, L., Li, G., Jiang, Z., Yau, K.-W., 2023. Unusual phototransduction via cross-motif
583 signaling from G_q to adenylyl cyclase in intrinsically photosensitive retinal ganglion cells.
584 *Proc. Natl. Acad. Sci.* 120, 2017. <https://doi.org/10.1073/pnas.2216599120>

585 Del Pilar Gomez, M.D.P., Nasi, E., 2000. Light transduction in invertebrate hyperpolarizing
586 photoreceptors: Possible involvement of a G(o)-regulated guanylate cyclase. *J. Neurosci.*
587 20, 5254–5263. <https://doi.org/10.1523/jneurosci.20-14-05254.2000>

588 Dexter, P.M., Lobanova, E.S., Finkelstein, S., Spencer, W.J., Skiba, N.P., Arshavsky, V.Y.,
589 2018. Transducin β -subunit can interact with multiple g protein γ -subunits to enable light
590 detection by rod photoreceptors. *eNeuro* 5, 1–9. <https://doi.org/10.1523/ENEURO.0144-18.2018>

591 Dizhoor, A.M., Lowe, D.G., Olshevskaya, E. V., Laura, R.P., Hurley, J.B., 1994. The human
592 photoreceptor membrane guanylyl cyclase, RetGC, is present in outer segments and is
593 regulated by calcium and a soluble activator. *Neuron* 12, 1345–1352.
594 [https://doi.org/10.1016/0896-6273\(94\)90449-9](https://doi.org/10.1016/0896-6273(94)90449-9)

595 Döring, C.C., Kumar, S., Tumu, S.C., Kourtesis, I., Hausen, H., 2020. The visual pigment
596 xenopsin is widespread in protostome eyes and impacts the view on eye evolution. *Elife* 9,
597 1–23. <https://doi.org/10.7554/ELIFE.55193>

598 Ekström, P., Garm, A., Pålsson, J., Vihtelic, T.S., Nilsson, D.E., 2008. Immunohistochemical
599 evidence for multiple photosystems in box jellyfish. *Cell Tissue Res.* 333, 115–124.
600 <https://doi.org/10.1007/s00441-008-0614-8>

601 Fain, G.L., Hardie, R., Laughlin, S.B., 2010. Phototransduction and the Evolution of
602 Photoreceptors. *Curr. Biol.* 20, R114–R124. <https://doi.org/10.1016/j.cub.2009.12.006>

603 Faurobert, E., Chen, C.K., Hurley, J.B., Teng, D.H.F., 1996. Drosophila neurocalcin, a fatty
604 acylated, Ca²⁺-binding protein that associates with membranes and inhibits in Vitro
605 phosphorylation of bovine rhodopsin. *J. Biol. Chem.* 271, 10256–10262.
606 <https://doi.org/10.1074/jbc.271.17.10256>

607 Firestein, S., 2001. How the olfactory system makes sense of scents. *Nature* 413, 211–218.
608 <https://doi.org/10.1038/35093026>

609 Gold, D.A., Katsuki, T., Li, Y., Yan, X., Regulski, M., Ibberson, D., Holstein, T., Steele, R.E.,
610 Jacobs, D.K., Greenspan, R.J., 2019. The genome of the jellyfish *Aurelia* and the evolution
611 of animal complexity. *Nat. Ecol. Evol.* 3, 96–104. <https://doi.org/10.1038/s41559-018-0719-8>

612 Gornik, S.G., Bergheim, B.G., Morel, B., Stamatakis, A., Foulkes, N.S., Guse, A., 2021.
613 Photoreceptor Diversification Accompanies the Evolution of Anthozoa. *Mol. Biol. Evol.* 38,
614 1744–1760. <https://doi.org/10.1093/molbev/msaa304>

615 Gurevich, E. V., Gurevich, V. V., 2006. Arrestins: Ubiquitous regulators of cellular signaling
616 pathways. *Genome Biol.* 7. <https://doi.org/10.1186/gb-2006-7-9-236>

617 Hardie, R.C., Raghu, P., 2001. Visual transduction in *Drosophila*. *Nature*.
618 <https://doi.org/10.1038/35093002>

619 Hattar, S., Lucas, R.J., Mrosovsky, N., Thompson, S., Douglas, R.H., Hankins, M.W., Lem, J.,
620 Biel, M., Hofmann, F., Foster, R.G., Yau, K.W., 2003. Melanopsin and rod–cone
621 photoreceptive systems account for all major accessory visual functions in mice. *Nature*
622 424, 76–81. <https://doi.org/10.1038/nature01761>

623 Ikura, M., 1996. Calcium binding and conformational response in EF-hand proteins. *Trends
624 Biochem. Sci.* 21, 14–17. [https://doi.org/10.1016/S0968-0004\(06\)80021-6](https://doi.org/10.1016/S0968-0004(06)80021-6)

625 Katoh, K., Standley, D.M., 2013. MAFFT multiple sequence alignment software version 7:
626 Improvements in performance and usability. *Mol. Biol. Evol.* 30, 772–780.
627 <https://doi.org/10.1093/molbev/mst010>

628 Katz, B., Minke, B., 2009. *Drosophila* photoreceptors and signaling mechanisms. *Front. Cell.
629 Neurosci.* 3, 2. <https://doi.org/10.3389/neuro.03.002.2009>

630 Kayal, E., Bentlage, B., Sabrina Pankey, M., Ohdera, A.H., Medina, M., Plachetzki, D.C.,

633 Collins, A.G., Ryan, J.F., 2018. Phylogenomics provides a robust topology of the major
634 cnidarian lineages and insights on the origins of key organismal traits. *BMC Evol. Biol.* 18,
635 1–18. <https://doi.org/10.1186/s12862-018-1142-0>

636 Koch, K.W., Stryer, L., 1988. Highly cooperative feedback control of retinal rod guanylate
637 cyclase by calcium ions. *Nature* 334, 64–66. <https://doi.org/10.1038/334064a0>

638 Kojima, D., Terakita, A., Ishikawa, T., Tsukahara, Y., Maeda, A., Shichida, Y., 1997. A novel
639 G(o)-mediated phototransduction cascade in scallop visual cells. *J. Biol. Chem.* 272,
640 22979–22982. <https://doi.org/10.1074/jbc.272.37.22979>

641 Koyanagi, M., Takano, K., Tsukamoto, H., Ohtsu, K., Tokunaga, F., Terakita, A., 2008. Jellyfish
642 vision starts with cAMP signaling mediated by opsin-Gs cascade. *Proc. Natl. Acad. Sci. U.*
643 *S. A.* 105, 15576–15580. <https://doi.org/10.1073/pnas.0806215105>

644 Kozmík, Z., Ruzicková, J., Jonasová, K., Matsumoto, Y., Vopalenský, P., Kozmíková, I., Strnad,
645 H., Kawamura, S., Piatigorský, J., Paces, V., Vlček, C., 2008. Assembly of the cnidarian
646 camera-type eye from vertebrate-like components. *Proc. Natl. Acad. Sci.* 105, 8989–8993.
647 <https://doi.org/10.1073/pnas.0800388105>

648 Krishnan, A., Mustafa, A., Almén, M.S., Fredriksson, R., Williams, M.J., Schiöth, H.B., 2015.
649 Evolutionary hierarchy of vertebrate-like heterotrimeric G protein families. *Mol. Phylogenet.*
650 *Evol.* 91, 27–40. <https://doi.org/10.1016/j.ympev.2015.05.009>

651 Lagman, D., Haines, H.J., Abalo, X.M., Larhammar, D., 2022. Ancient multiplicity in cyclic
652 nucleotide-gated (CNG) cation channel repertoire was reduced in the ancestor of
653 Olfactores before re-expansion by whole genome duplications in vertebrates. *PLoS One*
654 17, 1–27. <https://doi.org/10.1371/journal.pone.0279548>

655 Lagman, D., Sundström, G., Daza, D.O., Abalo, X.M., Larhammar, D., 2012. Expansion of
656 transducin subunit gene families in early vertebrate tetraploidizations. *Genomics* 100, 203–
657 211. <https://doi.org/10.1016/j.ygeno.2012.07.005>

658 Lamb, T.D., 2013. Evolution of phototransduction, vertebrate photoreceptors and retina. *Prog.*
659 *Retin. Eye Res.* 36, 52–119. <https://doi.org/10.1016/j.preteyeres.2013.06.001>

660 Lamb, T.D., Hunt, D.M., 2017. Evolution of the vertebrate phototransduction cascade activation
661 steps. *Dev. Biol.* 431, 77–92. <https://doi.org/10.1016/j.ydbio.2017.03.018>

662 Lamb, T.D., Patel, H.R., Chuah, A., Hunt, D.M., 2018. Evolution of the shut-off steps of
663 vertebrate phototransduction. *Open Biol.* 8, 170232. <https://doi.org/10.1098/rsob.170232>

664 Layden, M.J., Rentzsch, F., Röttinger, E., 2016. The rise of the starlet sea anemone
665 *Nematostella vectensis* as a model system to investigate development and regeneration.
666 *Wiley Interdiscip. Rev. Dev. Biol.* 5, 408–428. <https://doi.org/10.1002/wdev.222>

667 Lee, S.J., Xu, H., Montell, C., 2004. Rhodopsin kinase activity modulates the amplitude of the
668 visual response in *Drosophila*. *Proc. Natl. Acad. Sci. U. S. A.* 101, 11874–11879.
669 <https://doi.org/10.1073/pnas.0402205101>

670 Letunic, I., Bork, P., 2021. Interactive tree of life (iTOL) v5: An online tool for phylogenetic tree
671 display and annotation. *Nucleic Acids Res.* 49, W293–W296.
672 <https://doi.org/10.1093/nar/gkab301>

673 Levay, K., Cabrera, J.L., Satpaev, D.K., Slepak, V.Z., 1999. G β 5 prevents the RGS7-G α _o
674 interaction through binding to a distinct G γ -like domain found in RGS7 and other RGS
675 proteins. *Proc. Natl. Acad. Sci. U. S. A.* 96, 2503–2507.
676 <https://doi.org/10.1073/pnas.96.5.2503>

677 Liegertová, M., Pergner, J., Kozmíková, I., Fabian, P., Pombinho, A.R., Strnad, H., Pačes, J.,
678 Vlček, Č., Bartuňek, P., Kozmík, Z., 2015. Cubozoan genome illuminates functional
679 diversification of opsins and photoreceptor evolution. *Sci. Rep.* 5, 1–19.
680 <https://doi.org/10.1038/srep11885>

681 Lokits, A.D., Indrischek, H., Meiler, J., Hamm, H.E., Stadler, P.F., 2018. Tracing the evolution of
682 the heterotrimeric G protein α subunit in Metazoa. *BMC Evol. Biol.* 18, 1–27.
683 <https://doi.org/10.1186/s12862-018-1147-8>

684 Lyubarsky, A.L., Chen, C.K., Simon, M.I., Pugh, E.N., 2000. Mice lacking G-protein receptor
685 kinase 1 have profoundly slowed recovery of cone-driven retinal responses. *J. Neurosci.*
686 20, 2209–2217. <https://doi.org/10.1523/jneurosci.20-06-02209.2000>

687 Macias-Munoz, A., Murad, R., Mortazavi, A., 2019. Molecular evolution and expression of opsin
688 genes in *Hydra vulgaris*. *BMC Genomics* 20, 1–19. <https://doi.org/10.1186/s12864-019-6349-y>

689 Makino, E.R., Handy, J.W., Li, T., Arshavsky, V.Y., 1999. The GTPase activating factor for
690 transducin in rod photoreceptors is the complex between RGS9 and type 5 G protein β
691 subunit. *Proc. Natl. Acad. Sci. U. S. A.* 96, 1947–1952.
692 <https://doi.org/10.1073/pnas.96.5.1947>

693 Mason, B., Schmale, M., Gibbs, P., Miller, M.W., Wang, Q., Levay, K., Shestopalov, V., Slepak,
694 V.Z., 2012. Evidence for Multiple Phototransduction Pathways in a Reef-Building Coral.
695 *PLoS One* 7, 1–9. <https://doi.org/10.1371/journal.pone.0050371>

696 McCulloch, K., Liu, A., Babonis, L., Daly, C., Martindale, M.Q., Koenig, K., 2023. *Nematostella*
697 *vectensis* exemplifies the exceptional expansion and diversity of opsins in the eyeless
698 Hexacorallia. *bioRxiv* 2023.05.17. <https://doi.org/10.1101/2023.05.17.541201>

699 Minh, B.Q., Schmidt, H.A., Chernomor, O., Schrempf, D., Woodhams, M.D., Von Haeseler, A.,
700 Lanfear, R., Teeling, E., 2020. IQ-TREE 2: New Models and Efficient Methods for
701 Phylogenetic Inference in the Genomic Era. *Mol. Biol. Evol.* 37, 1530–1534.
702 <https://doi.org/10.1093/molbev/msaa015>

703 Montell, C., 2005. TRP channels in *Drosophila* photoreceptor cells. *J. Physiol.* 567, 45–51.
704 <https://doi.org/10.1111/jphysiol.2005.092551>

705 Moroz, L.L., Mukherjee, K., Romanova, D.Y., 2023. Nitric oxide signaling in ctenophores. *Front.*
706 *Neurosci.* 17, 1–15. <https://doi.org/10.3389/fnins.2023.1125433>

707 Ohdera, A., Ames, C.L., Dikow, R.B., Kayal, E., Chiodin, M., Busby, B., La, S., Pirro, S., Collins,
708 A.G., Medina, M., Ryan, J.F., 2019. Box, stalked, and upside-down? Draft genomes from
709 diverse jellyfish (cnidaria, acraspeda) lineages: *Alatina alata* (cubozoa), *calvadosia*
710 *cruxmelitensis* (staurozoa), and *cassiopea xamachana* (scyphozoa). *Gigascience* 8, 1–15.
711 <https://doi.org/10.1093/gigascience/giz069>

712 Okada, T., Sugihara, M., Bondar, A.N., Elstner, M., Entel, P., Buss, V., 2004. The retinal
713 conformation and its environment in rhodopsin in light of a new 2.2 Å crystal structure. *J.*
714 *Mol. Biol.* 342, 571–583. <https://doi.org/10.1016/j.jmb.2004.07.044>

715 Oldham, W.M., Hamm, H.E., 2006. Structural basis of function in heterotrimeric G proteins. *Q.*
716 *Rev. Biophys.* 39, 117–166. <https://doi.org/10.1017/S0033583506004306>

717 Palczewski, K., Kumada, T., Hori, T., Behnke, C.A., Motoshima, H., Fox, B.A., Trong, I. Le,
718 Teller, D.C., Okada, T., Stenkamp, R.E., Yamamoto, M., Miyano, M., 2000. Crystal
719 Structure of Rhodopsin: A G Protein-Coupled Receptor. *Science* 289, 739–745.
720 <https://doi.org/10.1126/science.289.5480.739>

721 Paysan-Lafosse, T., Blum, M., Chuguransky, S., Grego, T., Pinto, B.L., Salazar, G.A., Bileschi,
722 M.L., Bork, P., Bridge, A., Colwell, L., Gough, J., Haft, D.H., Letunić, I., Marchler-Bauer, A.,
723 Mi, H., Natale, D.A., Orengo, C.A., Pandurangan, A.P., Rivoire, C., Sigrist, C.J.A., Sillitoe,
724 I., Thanki, N., Thomas, P.D., Tosatto, S.C.E., Wu, C.H., Bateman, A., 2023. InterPro in
725 2022. *Nucleic Acids Res.* 51, D418–D427. <https://doi.org/10.1093/nar/gkac993>

726 Peng, G., Shi, X., Kadowaki, T., 2015. Evolution of TRP channels inferred by their classification
727 in diverse animal species. *Mol. Phylogenet. Evol.* 84, 145–157.
728 <https://doi.org/10.1016/j.ympev.2014.06.016>

729 Peng, Y.W., Robishaw, J.D., Levine, M.A., Yau, K.W., 1992. Retinal rods and cones have
730 distinct G protein β and γ subunits. *Proc. Natl. Acad. Sci. U. S. A.* 89, 10882–10886.
731 <https://doi.org/10.1073/pnas.89.22.10882>

732 Plachetzki, D.C., Fong, C.R., Oakley, T.H., 2012. Cnidocyte discharge is regulated by light and
733 opsin-mediated phototransduction. *BMC Biol.* 10. <https://doi.org/10.1186/1741-7007-10-17>

734

735 Plachetzki, D.C., Fong, C.R., Oakley, T.H., 2010. The evolution of phototransduction from an
736 ancestral cyclic nucleotide gated pathway. *Proc. R. Soc. B Biol. Sci.* 277, 1963–1969.
737 <https://doi.org/10.1098/rspb.2009.1797>

738 Potter, L.R., 2011. Guanylyl cyclase structure, function and regulation. *Cell. Signal.* 23, 1921–
739 1926. <https://doi.org/10.1016/j.cellsig.2011.09.001>

740 Premont, R.T., Koch, W.J., Inglese, J., Lefkowitz, R.J., 1994. Identification, purification, and
741 characterization of GRK5, a member of the family of G protein-coupled receptor kinases. *J.*
742 *Biol. Chem.* 269, 6832–6841. [https://doi.org/10.1016/s0021-9258\(17\)37451-3](https://doi.org/10.1016/s0021-9258(17)37451-3)

743 Price, M.N., Dehal, P.S., Arkin, A.P., 2010. FastTree 2 - Approximately maximum-likelihood
744 trees for large alignments. *PLoS One* 5. <https://doi.org/10.1371/journal.pone.0009490>

745 Ramirez, M.D., Pairett, A.N., Pankey, M.S., Serb, J.M., Speiser, D.I., Swafford, A.J., Oakley,
746 T.H., 2016. The last common ancestor of most bilaterian animals possessed at least nine
747 opsins. *Genome Biol. Evol.* 8, 3640–3652. <https://doi.org/10.1093/gbe/evw248>

748 Rawlinson, K.A., Lapraz, F., Ballister, E.R., Terasaki, M., Rodgers, J., McDowell, R.J.,
749 Girstmair, J., Criswell, K.E., Boldogkoi, M., Simpson, F., Goulding, D., Cormie, C., Hall, B.,
750 Lucas, R.J., Telford, M.J., 2019. Extraocular, rod-like photoreceptors in a flatworm express
751 xenopsin photopigment. *Elife* 8, 1–28. <https://doi.org/10.7554/elife.45465>

752 Schnitzler, C.E., Pang, K., Powers, M.L., Reitzel, A.M., Ryan, J.F., Simmons, D., Tada, T., Park,
753 M., Gupta, J., Brooks, S.Y., Blakesley, R.W., Yokoyama, S., Haddock, S.H.D., Martindale,
754 M.Q., Baxevanis, A.D., 2012. Genomic organization, evolution, and expression of
755 photoprotein and opsin genes in *Mnemiopsis leidyi*: A new view of ctenophore photocytes.
756 *BMC Biol.* 10. <https://doi.org/10.1186/1741-7007-10-107>

757 Sebé-Pedrós, A., Saudemont, B., Chomsky, E., Plessier, F., Mailhé, M.P., Renno, J., Loe-Mie,
758 Y., Lifshitz, A., Mukamel, Z., Schmutz, S., Novault, S., Steinmetz, P.R.H., Spitz, F., Tanay,
759 A., Marlow, H., 2018. Cnidarian Cell Type Diversity and Regulation Revealed by Whole-
760 Organism Single-Cell RNA-Seq. *Cell* 173, 1520–1534.e20.
761 <https://doi.org/10.1016/j.cell.2018.05.019>

762 Shichida, Y., Matsuyama, T., 2009. Evolution of opsins and phototransduction. *Philos. Trans. R.*
763 *Soc. B Biol. Sci.* 364, 2881–2895. <https://doi.org/10.1098/rstb.2009.0051>

764 Simon, M.I., Strathmann, M.P., Gautam, N., 1991. Diversity of G proteins in signal transduction.
765 *Science* (80-). 252, 802–808. <https://doi.org/10.1126/science.1902986>

766 Squires, K.E., Montañez-Miranda, C., Pandya, R.R., Torres, M.P., Hepler, J.R., 2018. Genetic
767 analysis of rare human variants of regulators of G protein signaling proteins and their role
768 in human physiology and disease. *Pharmacol. Rev.* 70, 446–474.
769 <https://doi.org/10.1124/pr.117.015354>

770 Suga, H., Schmid, V., Gehring, W.J., 2008. Evolution and Functional Diversity of Jellyfish
771 Opsins. *Curr. Biol.* 18, 51–55. <https://doi.org/10.1016/j.cub.2007.11.059>

772 Sun, Z.L., Zheng, Y.H., Liu, W., 2018. Identification and characterization of a novel calmodulin
773 binding site in Drosophila TRP C-terminus. *Biochem. Biophys. Res. Commun.* 501, 434–
774 439. <https://doi.org/10.1016/j.bbrc.2018.05.007>

775 Swardfager, W., Mitchell, J., 2007. Purification of visual arrestin from squid photoreceptors and
776 characterization of arrestin interaction with rhodopsin and rhodopsin kinase. *J. Neurochem.*
777 101, 223–231. <https://doi.org/10.1111/j.1471-4159.2006.04364.x>

778 Tanaka, T., Ames, J.B., Harvey, T.S., Stryer, L., Ikura, M., 1995. Sequestration of the
779 membrane-targeting myristoyl group of recoverin in the calcium-free state. *Nature* 376,
780 444–447. <https://doi.org/10.1038/376444a0>

781 Tarrant, A.M., Helm, R.R., Levy, O., Rivera, H.E., 2019. Environmental entrainment
782 demonstrates natural circadian rhythmicity in the cnidarian *Nematostella vectensis*. *J. Exp.*
783 *Biol.* 222. <https://doi.org/10.1242/jeb.205393>

784 Terakita, A., 2005. The opsins. *Genome Biol.* 6, 1–9. <https://doi.org/10.1186/gb-2005-6-3-213>

785 Trudeau, M.C., Zagotta, W.N., 2004. Dynamics of Ca²⁺-calmodulin-dependent inhibition of rod

786 cyclic nucleotide-gated channels measured by patch-clamp fluorometry. *J. Gen. Physiol.*
787 124, 211–223. <https://doi.org/10.1085/jgp.200409101>

788 Velarde, R.A., Sauer, C.D., Walden, K.K.O., Fahrbach, S.E., Robertson, H.M., 2005. Pteropsin:
789 A vertebrate-like non-visual opsin expressed in the honey bee brain. *Insect Biochem. Mol.*
790 *Biol.* 35, 1367–1377. <https://doi.org/10.1016/j.ibmb.2005.09.001>

791 Vöcking, O., Kourtesis, I., Tumu, S.C., Hausen, H., 2017. Co-expression of xenopsin and
792 rhabdomeric opsin in photoreceptors bearing microvilli and cilia. *eLife* 6, 1–26.
793 <https://doi.org/10.7554/eLife.23435>

794 Vöcking, O., Macias-Muñoz, A., Jaeger, S.J., Oakley, T.H., 2022. Deep Diversity: Extensive
795 Variation in the Components of Complex Visual Systems across Animals. *Cells* 11, 3966.
796 <https://doi.org/10.3390/cells11243966>

797 Wang, T., Montell, C., 2007. Phototransduction and retinal degeneration in *Drosophila*. *Pflugers
798 Arch. Eur. J. Physiol.* 454, 821–847. <https://doi.org/10.1007/s00424-007-0251-1>

799 Warner, J.F., Guerlais, V., Amiel, A.R., Johnston, H., Nedoncelle, K., Röttinger, E., 2018.
800 NvERTx: a gene expression database to compare embryogenesis and regeneration in the
801 sea anemone *Nematostella vectensis*. *Development* 145, dev162867.
802 <https://doi.org/10.1242/dev.162867>

803 Wilden, U., Hall, S.W., Kuhn, H., 1986. Phosphodiesterase activation by photoexcited rhodopsin
804 is quenched when rhodopsin is phosphorylated and binds the intrinsic 48-kDa protein of
805 rod outer segments. *Proc. Natl. Acad. Sci. U. S. A.* 83, 1174–1178.
806 <https://doi.org/10.1073/pnas.83.5.1174>

807 Yamashita, T., Ohuchi, H., Tomonari, S., Ikeda, K., Sakai, K., Shichida, Y., 2010. Opn5 is a UV-
808 sensitive bistable pigment that couples with Gi subtype of G protein. *Proc. Natl. Acad. Sci.
809 U. S. A.* 107, 22084–22089. <https://doi.org/10.1073/pnas.1012498107>

810 Yau, K.W., 1994. Phototransduction mechanism in retinal rods and cones. The Friedenwald
811 lecture. *Investig. Ophthalmol. Vis. Sci.* 35, 9–32.

812 Yau, K.W., Hardie, R.C., 2009. Phototransduction Motifs and Variations. *Cell* 139, 246–264.
813 <https://doi.org/10.1016/j.cell.2009.09.029>

814 Zimmermann, B., Robb, S.M.C., Genikhovich, G., Fropf, W.J., Weilguny, L., He, S., Chen, S.,
815 Lovegrove-Walsh, J., Hill, E.M., Ragkousi, K., Praher, D., Fredman, D., Moran, Y., Gibson,
816 M.C., Technau, U., 2020. Sea anemone genomes reveal ancestral metazoan chromosomal
817 macrosynteny. *bioRxiv* 2020.10.30.359448. <https://doi.org/10.1101/2020.10.30.359448>

818

819

820 **Tables and Figures**

821

Table 1. Presence of phototransduction cascade orthologs in representative species

Species	Opsin #	G alpha #	Effector enzyme #	Channel #
c-opsin cascade	c-opsin	Gai/t	PDE6	CNG
<i>M. musculus</i>	4	2	3	6
Insect	1	1	1	4
<i>N. vectensis</i>	15	1	1	5
<i>H. vulgaris</i>	0	1	1	1
r-opsin cascade	r-opsin	Gaq	PLC beta	TRPC
<i>M. musculus</i>	1	1	1	7
Insect	7	1	2	3
<i>N. vectensis</i>	0 (2*)	1	2	8
<i>H. vulgaris</i>	0 (0*)	1	3	1

822 * ASO-I opsins, which in some phylogenetic hypotheses are sister to r-opsins, though this relationship is still debated.

823

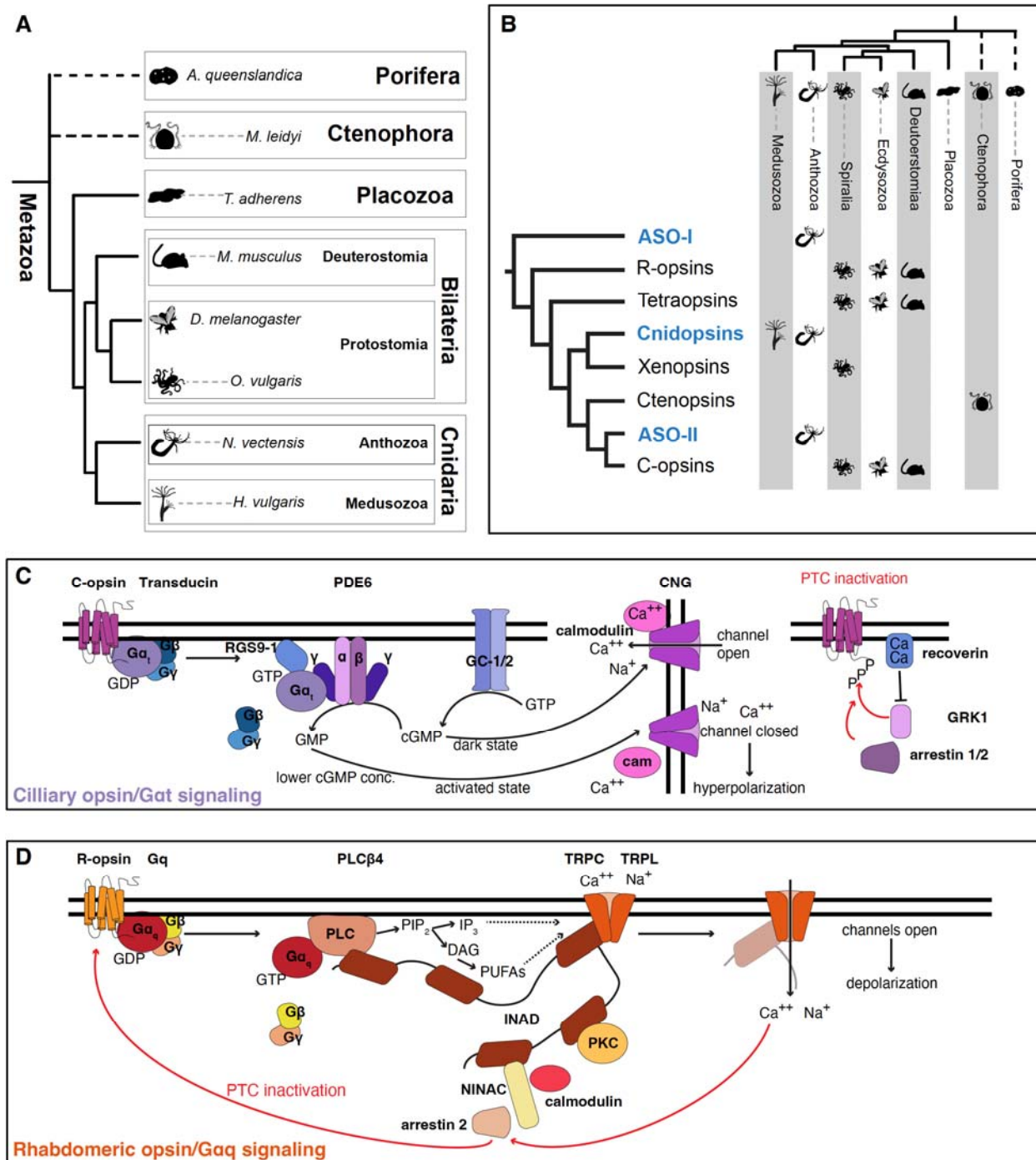
824

Table 2. Summary of phototransduction homologs in representative species

Gene	<i>M. leidyi</i>	<i>H. vulgaris</i>	<i>N. vectensis</i>	<i>M. musculus</i>	<i>D. melanogaster</i>
TRPC	1	1	8	7	3
TRPM	0	6	3	8	1
GC	2	2	6	3	5
AC	2	4	3	8	12
ANPR	1	2	3	3	0
Arrestin	1	1	1	4	3
CNG	2	1	5	6	4
GMP-PDE	3	5	5	6	4
G alpha	11	4	6	17	8
G beta	3	2	2	5	2
G gamma	1	4	5	14	3
PLC	1	3	2	4	2
GRKs	2	2	2	4	2
RGS (R-7 family)	1	2	2	5	3

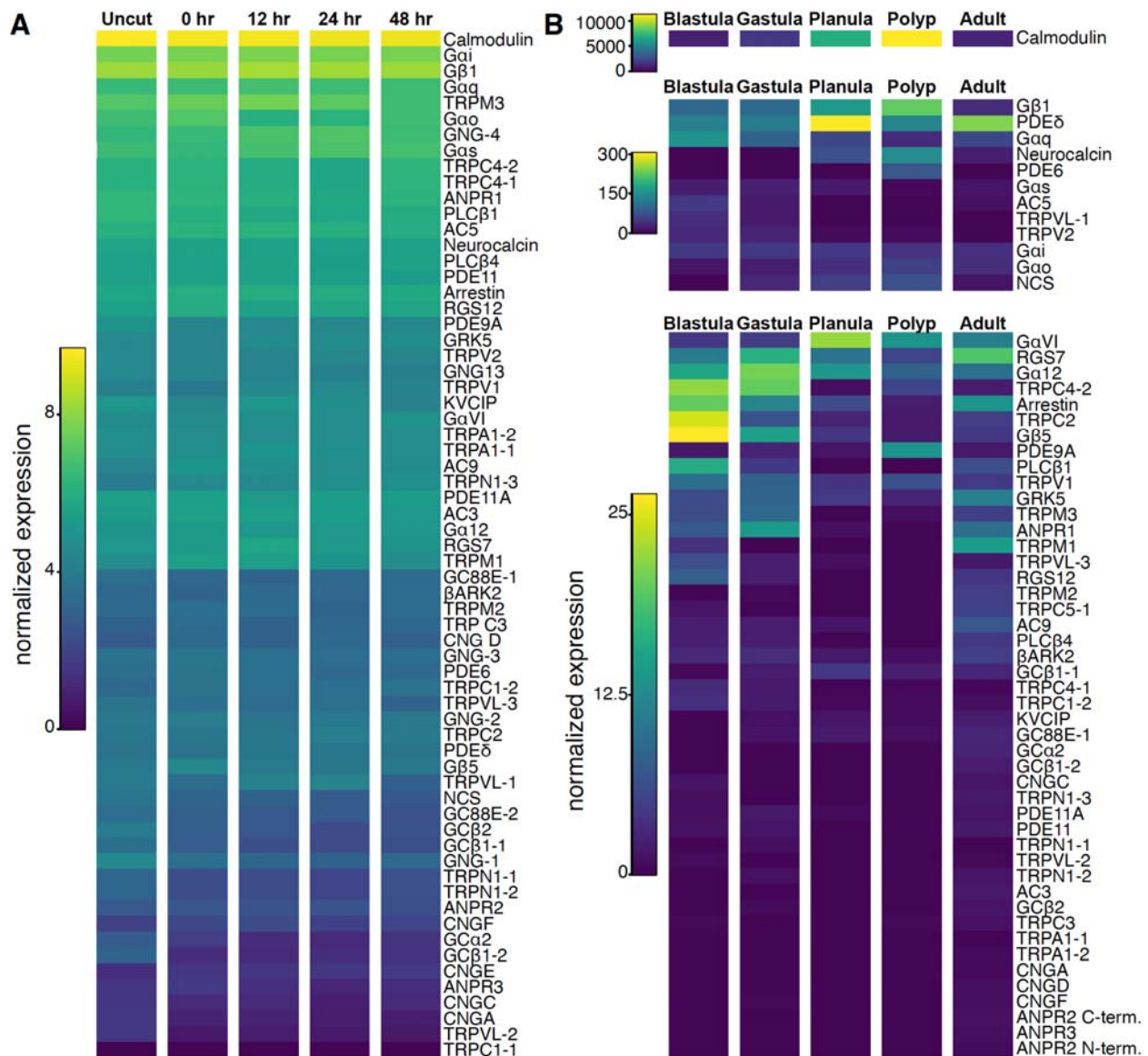
825

826

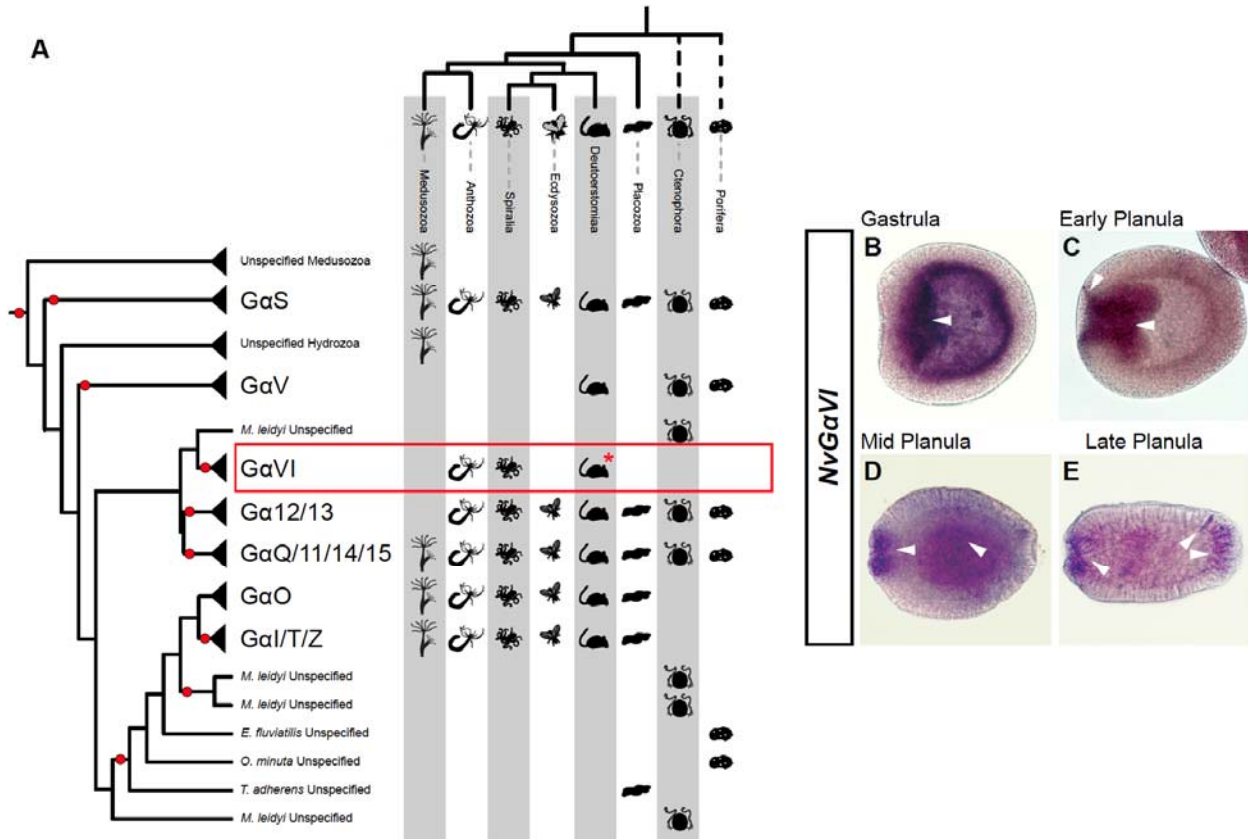


827
828
829
830
831
832
833
834
835
836

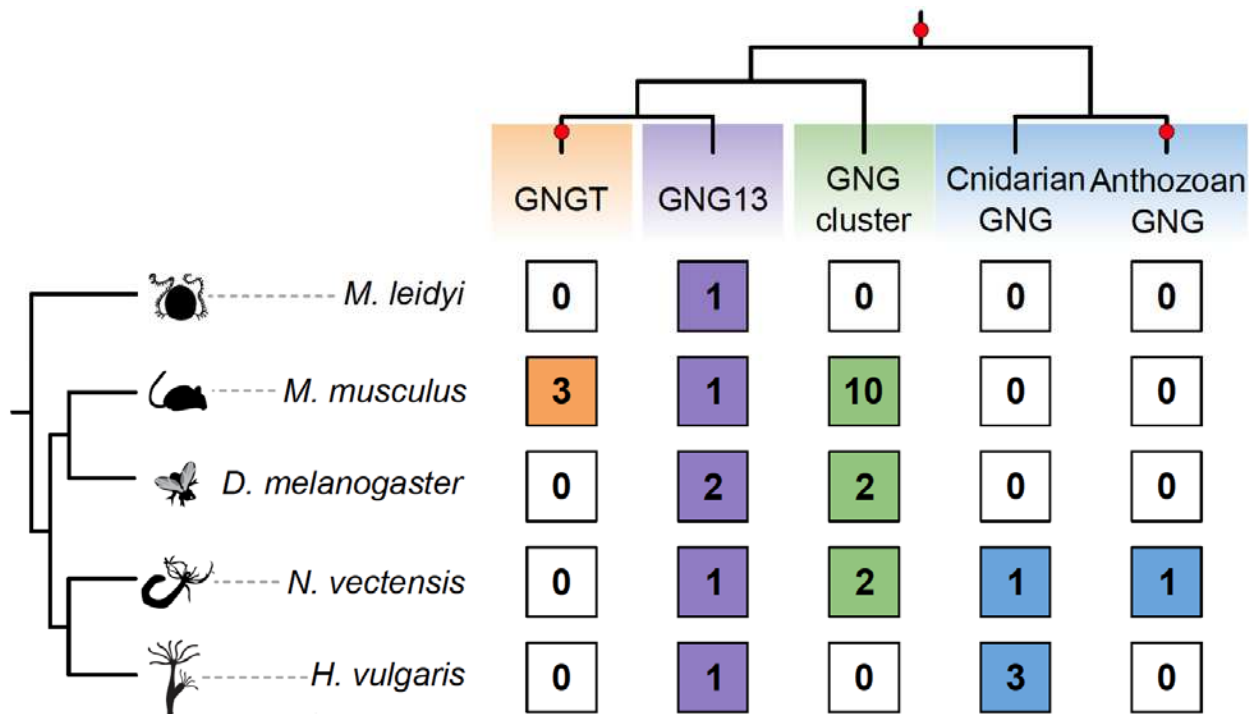
Figure 1. Major animal and opsin lineage relationships. **A)** Animal tree showing the major animal groups and the representative species from each group highlighted in this study. **B)** Current hypothesis of animal opsin relationships with presence or absence of each opsin group in each animal lineage indicated by the symbol. Cnidopsins and xenopsins together form a monophyletic clade, and ASO-II and c-opsins together form a monophyletic clade. Cnidarian-specific groups are highlighted in blue. Tree adapted from McCulloch et al. 2023. **C)** Schematic of the c-opsin phototransduction cascade and the proteins investigated in the current study. **D)** Schematic of the r-opsin phototransduction cascade and the proteins investigated in the current study.



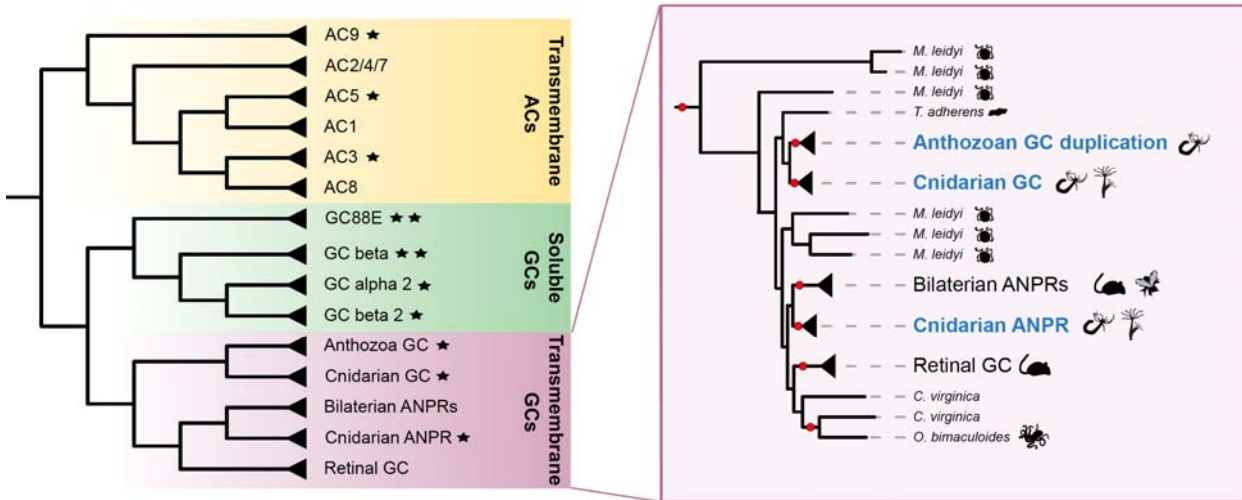
837
838 **Figure 2. mRNA expression levels of phototransduction genes in regeneration and**
839 **development. A)** Expression levels from timecourse series at different stages of whole
840 regenerating oral pole from NvERTx (Warner et al. 2015). **B)** Expression levels from timecourse
841 series at different stages of development from whole animals, from blastula to adult. Data is
842 from (McCulloch et al. 2023). Different scales are used for the top expressing genes for visual
843 clarity.
844



845
846 **Figure 3. G α subunit protein evolution in animals** **A)** Maximum-likelihood G α subunit tree
847 with major subgroups collapsed and individual branches from undefined sponge and ctenophore
848 sequences. Presence of each subfamily in each animal lineage is indicated by animal symbol. A
849 novel group, GaVI, is indicated by a red box. Asterisk, subunit is found in Deuterostomes, but
850 only found in *Branchiostoma*. Red circles indicate highly supported nodes with 80% aSH-
851 LRT/95% UFbs support. **B-E)** Spatial expression of the novel NvGaVI mRNA in *N. vectensis*
852 development. **B)** At gastrula stage, expression is highest in the pre-endodermal plate
853 (arrowhead) which is invaginating and is beginning to form the endoderm. **C)** By early planula
854 stage expression is around the lip of the mouth, the elongating pharynx ectoderm, and the
855 expanding endoderm (arrowheads). **D)** By mid planula expression is seen in the cells
856 surrounding the mouth and broadly in the interior endoderm (arrowheads). **E)** By late planula
857 expression is still found around the mouth, and in the sensory apical organ (arrowheads). Some
858 expression is still seen in broadly in the endoderm. In all panels, mouth is to the left, apical
859 organ/aboral to the right.
860

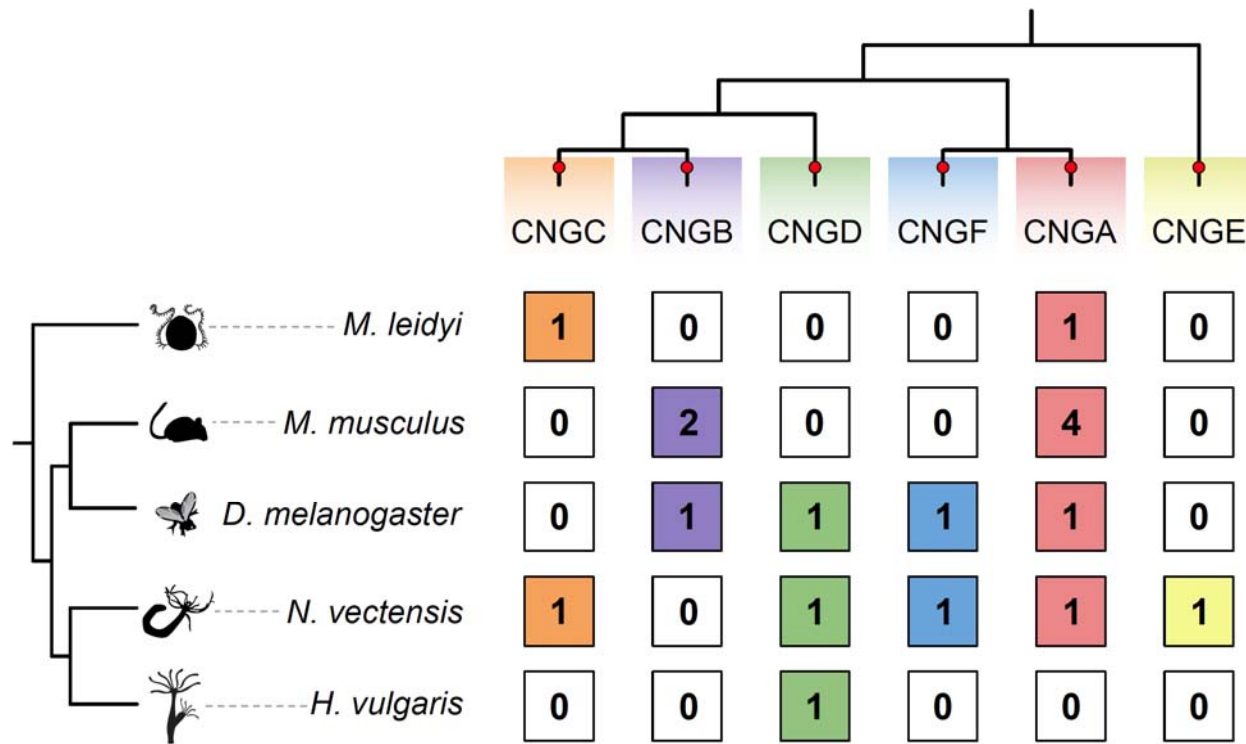


861
862 **Figure 4. G \square subunit protein family.** Simplified maximum-likelihood G \square tree with major
863 subgroups collapsed, top. The number of subfamily paralogs in each animal lineage is indicated
864 by numbers in colored boxes. Red circles indicate highly supported branches with 80% aSH-
865 LRT/95% UFbs support.
866



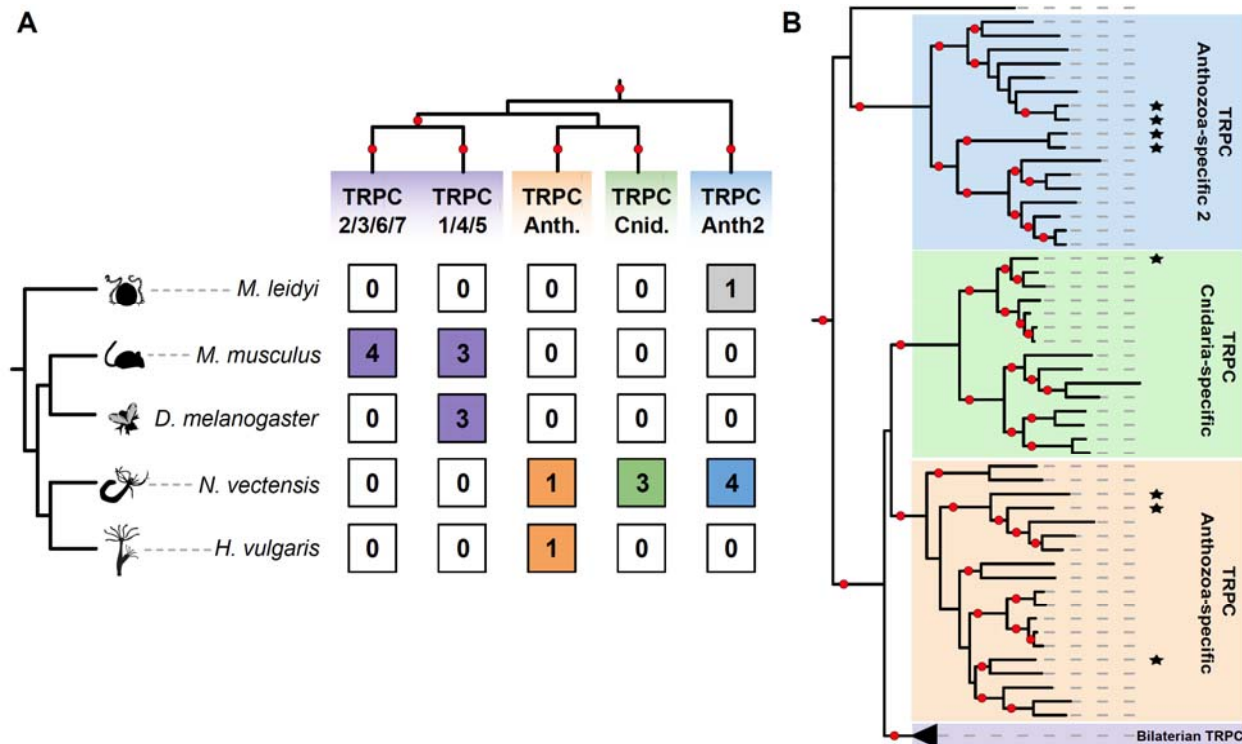
867
868
869
870
871
872
873
874

Figure 5. Anthozoan expansions in the AC/GC/ANPR protein family. A) Maximum-likelihood tree with major AC/GC/ANPR subgroups collapsed and individual branches with no clear group from Ctenophora, Placozoa, and Spiralia removed. **B)** Transmembrane GCS in the tree expanded, showing many orphans with no clear group from Ctenophora, Placozoan, and Spiralia. Groups in blue show cnidarian and anthozoan-specific groups. Red circles indicate highly supported branches with 80% aSH-LRT/95% UFbs support.



875
876
877
878
879
880

Figure 6. CNG subunit protein family. Simplified maximum-likelihood CNG tree with major subgroups collapsed, top. The number of subfamily paralogs in each animal lineage is indicated by numbers in colored boxes. Red circles indicate highly supported branches with 80% aSH-LRT/95% UFbs support.



881
882 **Figure 7. TRP channel evolution Anthozoa** **A)** Simplified maximum-likelihood TRPC tree with
883 major subgroups collapsed, top. The number of subfamily paralogs in each animal lineage is
884 indicated by numbers in colored boxes. Gray box is for the ctenophore sequence which is not
885 supported in any clade but is sister to the Anthozoa 2 group. **B)** Expanded maximum-likelihood
886 tree of TRPC subfamilies focused on cnidarian-specific expansions. Stars next to branches
887 indicate the *N. vectensis* sequences. Red circles indicate highly supported branches with 80%
888 aSH-LRT/95% UFbs support.

889